Domain-specific control of germ cell polarity and migration by multifunction Tre1 GPCR

Michelle G. LeBlanc[1,2] and Ruth Lehmann[1,2]

[1]Howard Hughes Medical Institute, Kimmel Center for Biology and Medicine of the Skirball Institute and [2]Department of Cell Biology, New York University School of Medicine, New York, NY

The migration of primordial germ cells (PGCs) from their place of origin to the embryonic gonad is an essential reproductive feature in many animal species. In *Drosophila melanogaster*, a single G protein–coupled receptor, Trapped in endoderm 1 (Tre1), mediates germ cell polarization at the onset of active migration and directs subsequent migration of PGCs through the midgut primordium. How these different aspects of cell behavior are coordinated through a single receptor is not known. We demonstrate that two highly conserved domains, the E/N/DRY and NPxxY motifs, have overlapping and unique functions in Tre1. The Tre1-NRY domain via G protein signaling is required for reading and responding to guidance and survival cues controlled by the lipid phosphate phosphatases Wunen and Wunen2. In contrast, the Tre1-NPIIY domain has a separate role in Rho1- and E-cadherin–mediated polarization at the initiation stage independent of G protein signaling. We propose that this bifurcation of the Tre1 G protein–coupled receptor signaling response via G protein–dependent and independent branches enables distinct spatiotemporal regulation of germ cell migration.

Introduction

Germ cell migration is a highly conserved process across species. Given the ease by which germ cells can be uniquely identified, primordial germ cell (PGC) migration has become a powerful model to dissect the process of directed, single-cell migration in multicellular organisms (Barton et al., 2016). In *Drosophila melanogaster*, germ cells form at the posterior pole of the embryo and are brought into the midgut primordium during gastrulation movements. Here germ cells migrate through the midgut epithelium, exposing them to attractive and repellent cues that guide them to the somatic gonadal precursors. Genetic screens have identified numerous genes that regulate germ cell migration (reviewed by Richardson and Lehmann, 2010). Among them, the G protein–coupled receptor (GPCR) Trapped in endoderm 1 (Tre1) is required for the initial polarization and individualization of germ cells and their subsequent migration out of the posterior midgut primordium. Germ cells lacking Tre1 fail to initiate migration and remain clustered within the midgut primordium throughout embryogenesis (Kunwar et al., 2003, 2008). A hypomorphic allele of *tre1*, known as $tre1^{sctt}$, revealed an additional phenotype whereby many cells exit the midgut but fail to migrate to the somatic gonad (Coffman et al., 2002; Kunwar et al., 2003). These data suggest that Tre1 is required not only at the start of migration but also during migration upon midgut exit.

Tre1 is an orphan receptor, and its signaling pathways have not been clearly delineated. Previous studies analyzing the function of Tre1 in neuroblast polarity identified G protein α o (Gαo) as a downstream signaling component (Yoshiura et al., 2012). Similarly, G protein α i/o (Gαi/o), mediates signaling by a close homologue of Tre1, Moody, in establishing the blood-brain barrier in *Drosophila* (Schwabe et al., 2005). Other genes with migratory phenotypes similar to Tre1 have provided valuable insight into the possible mechanisms that may cooperate with Tre1 to provide faithful guidance to germ cells. Indeed, mutations in the lipid phosphate phosphatase (LPP) Wunen (Wun) and its homologue Wun2 result in migration phenotypes strikingly similar to *tre1*. (Because of their exchangeable function, we will hereafter refer to Wun and Wun2 collectively as Wunen unless specifically noted.) Wunen LPP activity is required both in the germ cells and in specific somatic tissues for germ cell dispersal, survival, and migration (Zhang et al., 1996; Hanyu-Nakamura et al., 2004; Renault et al., 2004, 2010). In the soma, Wun and Wun2 repel germ cells and thereby guide them toward the gonad. In the absence of both *wunen* genes in the somatic tissues of the embryo, germ cells fail to migrate toward the somatic gonad and instead scatter throughout the embryo, a phenotype similar to that observed for $tre1^{sctt}$ (Starz-Gaiano et al., 2001; Coffman et al., 2002; Kunwar et al., 2003; Renault et al., 2004). Maternally provided Wun2 is required autonomously

Correspondence to Ruth Lehmann: ruth.lehmann@med.nyu.edu

Abbreviations used: Gαo, G protein α o; GPCR, G protein–coupled receptor; LPP, lipid phosphate phosphatase; PAGFP, photoactivatable GFP; PGC, primordial germ cell; ROI, region of interest; S1P, sphingosine-1-phosphate; TM, transmembrane domain; Wun, Wunen.

The Rockefeller University Press
J. Cell Biol. Vol. 216 No. 9 2945–2958
https://doi.org/10.1083/jcb.201612053

in germ cells for their survival. Loss of maternal Wun and Wun2 prevents exit from the midgut, a phenotype reminiscent of the strong *tre1* phenotype (Hanyu-Nakamura et al., 2004; Renault et al., 2004, 2010). As lipid phosphatases, Wun and Wun 2 have been shown to hydrolyze phospholipids and to promote the uptake of the lipid product into cells (Renault et al., 2004). Taking available genetic data into account, it has been proposed that somatic and germ cells compete for the same phospholipid substrate with alternative outcomes for germ cells (Renault et al., 2004). Wunen-mediated hydrolysis of the phospholipid and uptake of lipid are required in germ cells for their survival and may also facilitate dispersion of germ cells by local germ cell–germ cell competition (Renault et al., 2010). In the soma, depletion of phospholipid by Wunen-expressing cells generates a gradient that guides germ cells toward higher levels of phospholipid (Renault et al., 2004). Local depletion of phospholipid because of high levels of Wunen activity in the soma causes PGC death, consistent with the phospholipid requirement for germ cell survival (Fig. S4 A). Although similarities between *tre1* and *wun*/*wun2* mutant migration phenotypes suggest that these genes work in the same pathway, such a connection has not been directly demonstrated and is a focus of this study.

Tre1 belongs to the class A, Rhodopsin family of G protein–coupled, seven transmembrane receptors. GPCRs contain conserved intramolecular switches that transfer receptor activation to downstream signaling pathways. Among these, the E/N/DRY motif at the cytoplasmic border of transmembrane domain (TM) 3 and the NPxxY peptide motif located at the end of TM7 are widely conserved (Probst et al., 1992; Gether, 2000). A recent comparative analysis of crystal structures of 27 class A receptors in either the active or inactive state highlights the importance of these domains and provides a more generalized view of GPCR regulation (Venkatakrishnan et al., 2016). In the inactive state, interactions between sequences in the cytoplasmic side of TM6 and sequences surrounding the E/N/DRY motif at the end of TM3 or the NPxxY motif of TM7 appear to stabilize the inactive receptor. Upon receptor activation, interhelical interactions within the receptor change, and TM6 moves away from the transmembrane helix bundle, allowing TM3 domains to engage with TM7. This new TM3/TM7 constellation presents the G protein active state (Rasmussen et al., 2011; Schwartz and Sakmar, 2011; Trzaskowski et al., 2012; Venkatakrishnan et al., 2016). In addition to a role in switching between the receptor inactive and activated state, additional roles for the NPxxY domain independently of G protein signaling have been reported. Studies in cell culture show that the NPxxY domain can directly bind to Rho1 independently of the G protein complex (Mitchell et al., 1998). Interestingly, Tre1 function is required for the polarization of Rho1 to the germ cell tail, and normal Rho1 activity is required for germ cell migration (Kunwar et al., 2003, 2008). Furthermore, recent work on the chemokine GPCR, CCR7, required for T cell migration, shows that the NPxxY domain acts as a scaffold to provide an interface for receptor oligomerization and an associated signaling function separable from its role in G protein signaling (Hauser et al., 2016).

Here we explore the roles of the conserved NRY and NPIIY domains of Tre1 GPCR in germ cell migration. For this in vivo structure-function analysis, we developed assays that allowed us to dissect the downstream response to receptor activation at the cellular level. We found that both domains are required for proper germ cell migration to the gonad, though neither domain is sufficient. Interestingly, we identified functional differences between the domains. The NRY domain mediates Wunen-specific directional migration and survival cues, while the NPIIY domain is required for germ cell polarization. The fact that we can identify functionally distinct domains mediated by the same GPCR strongly suggests that separate signaling pathways control the cellular response to Tre1 activation. Given the conserved nature and abundance of these motifs in a wide variety of GPCRs, our analysis provides new insight into the functional compartmentalization of receptor response at a cellular level.

Results

Conserved domains in Tre1 GPCR mediate germ cell migration

Tre1 shares the conserved NRY and NPIIY domains with other Rhodopsin family GPCRs. To address context-specific roles in Tre1-mediated germ cell migration, we generated transgenes carrying mutations in either or both domains (Fig. 1 A). To disrupt the NRY domain, the arginine in the NRY domain was mutated to alanine. This arginine is the most highly conserved amino acid of the NRY domain and has previously been shown to be essential for germ cell migration and is the causative mutation in the $tre1^{sctt}$ allele (Kamps et al., 2010). To disrupt the NPIIY motif, we mutated the asparagine and proline to alanines, as these residues had been previously implicated in Rho1 binding (Mitchell et al., 1998; Borroto-Escuela et al., 2011). Molecular dynamics simulations using the Tre1 receptor predicted that a salt bridge between TM6 and the NRY motif in TM3 potentially stabilized the inactive state (Pruitt et al., 2013). We therefore mutated the aspartic acid residue (D266A) implicated as critical for this interaction to test this prediction. Finally, we generated a *tre1* construct in which both motifs were disrupted, termed double mutant or $NRY^{-}NPIIY^{-}$. Flag, Myc doubly tagged and untagged versions of each construct were driven by the *nanos* promoter, regulated under *nanos* 5′UTR and 3′UTR, and inserted into the *Drosophila* genome using site-specific integration to allow comparable, germ line–specific gene expression among constructs. Protein expression levels were similar between mutant and wild-type *tre1* constructs (Fig. S1 A), and all transgenic TRE1 proteins localized to the germ cell membrane (Fig. S1 B). Germ cell migration was not altered by transgene expression in a $tre1^{+/+}$ background, suggesting that none of these constructs dominantly interferes with Tre1 wild-type function (Fig. S1 C).

To assess the impact of mutations in an individual domain on germ cell migration, transgenes were placed in a *tre1*-null mutant background. (For exact crossing schemes, refer to Table S1 and "Materials and methods"). The $tre1^{\Delta EP5}$ allele removes the first exon of *tre1* and has been shown to be void of *tre1* RNA in germ cells (Kunwar et al., 2003). Embryos derived from mutant $tre1^{\Delta EP5}$ mothers (hereafter referred to as mutant embryos) show striking defects in germ cell migration; most germ cells remain in the midgut and fail to migrate to the somatic gonad (Kunwar et al., 2003). Stage 13–15 embryos were stained for Vasa (germ cells) and Eya (somatic gonad precursors) and imaged using confocal microscopy, and the number of germ cells that reached the gonad was quantified as a percentage of the total. A tagged wild-type *tre1* control transgene fully restored normal germ cell migration, with more than 95% of germ cells per embryo reaching the gonad (95.2 ± 1.3% SEM, n = 14;

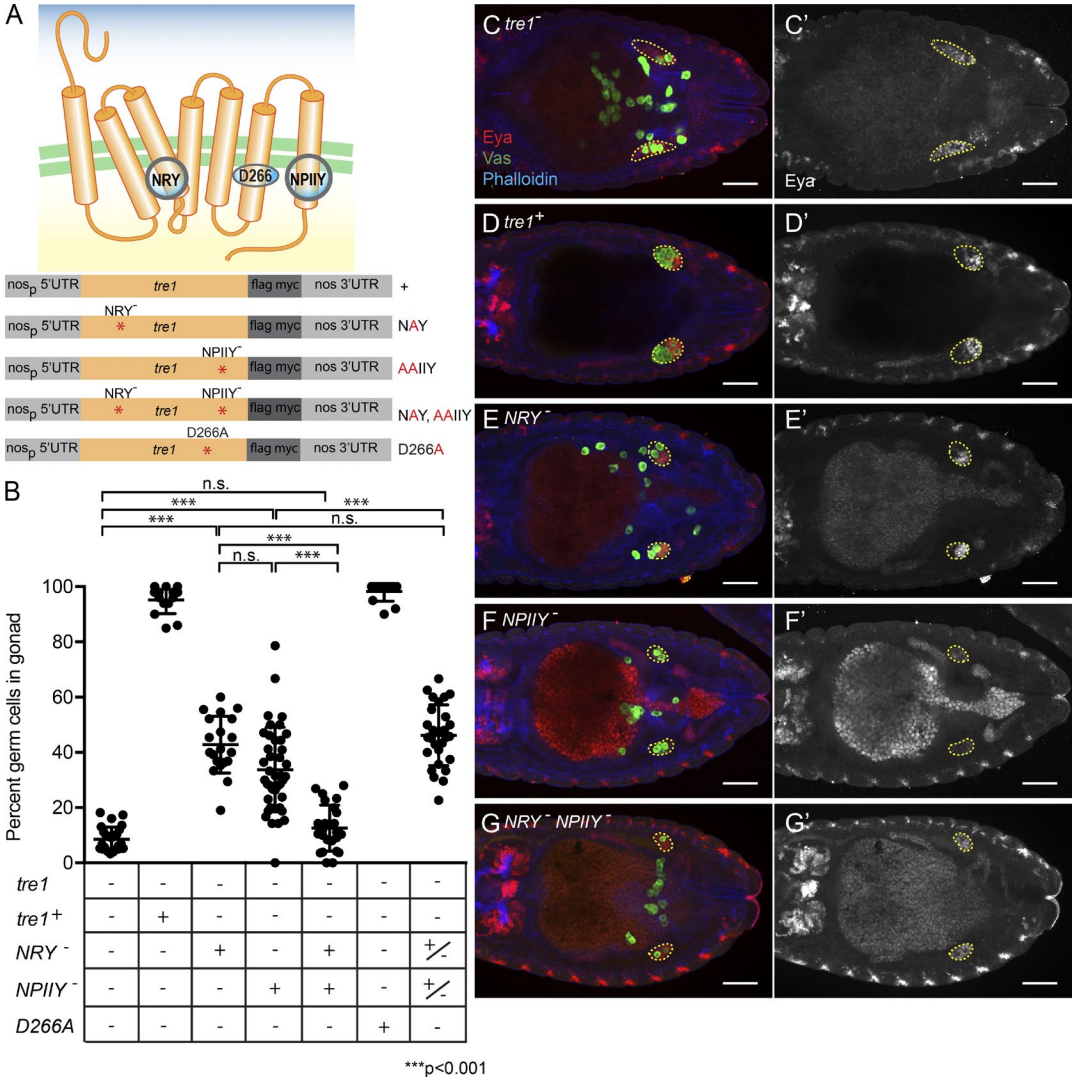

Figure 1. **Conserved domains in Tre1 GPCR are required for germ cell migration.** (A) Schematic drawing of Tre1 protein and the location of the conserved domains. Amino acid alterations are listed to the right in red. (B) Scatterplots showing number of germ cells in the gonad in each genotype as a percentage of the total. Error bars represent standard deviation; +/− indicates transheterozygotes. At least 20 embryos were analyzed per genotype. ***, P < 0.001. There is no significant difference between *tre1*-null and *tre1 NRY⁻NPIIY⁻*. (C–G) Representative images of embryos at stage 14 stained for Vasa (green, germ cells), Eya (somatic gonad, red; gray in C′–G′), and actin (phalloidin, blue). All embryos shown lack maternal and zygotic contribution of endogenous *tre1* gene, (*tre1⁻*) and inherited maternally provided Tre1 wild ype (*tre1⁺*; C) or mutated forms of the receptor expressed from the respective *tre1* transgene under *nanos* promoter, *nanos 5′* and *3′* UTRs (D–G). Bars, 50 µm. The somatic gonad is outlined in yellow hashes. For crossing schemes and genotypes, see Table S1.

Fig. 1, B and D). Germ cell migration was significantly disrupted in both *NRY* and *NPIIY* mutant embryos (42.8 ± 2.3%, n = 20, and 33.8 ± 2.4%, n = 40, respectively), though not as severely as in *tre1* loss-of-function mutants (8.6 ± 0.9%, n = 26; Fig. 1, B, C, E, and F). Interestingly, mutating the aspartic acid residue (D266A) that was predicted to stabilize the NRY/TM6 interaction in the inactive state had no effect on germ cell migration in a wild-type or mutant *tre1* background (98.8 ± 0.5%, n = 47, and 98.2 ± 1%, n = 13, respectively; Fig. 1, A and B; and Fig. S1 C). When placed in trans, the *NRY* and *NPI IY* domain mutants failed to restore normal migration (51.6 ± 2.3%, n = 16; Fig. 1 B). The phenotype was similar to the *NRY* single-domain mutants (Fig. 1 B), implying that the two domains share functions and that both are required to be active in the same molecule. The *NRY⁻NPIIY⁻* double mutant showed a stronger phenotype and recapitulated the *tre1*-null phenotype (12.6 ± 1.7%, n = 24; Fig. 1, B, C, and G). These results suggest that the NRY and NPIIY domains must also have separate roles that synergize to generate full Tre1 function and that these distinct roles are complemented in the single-domain mutants. To determine how individual Tre1 domains contribute to germ cell behavior at the cellular level, we used a set of assays to evaluate (a) the timing of germ cell exit from the midgut, (b) germ cell polarization at the onset of migration, (c) directional migration and midline avoidance during the migration to the somatic gonad, and (d) germ cell survival during migration.

Tre1 NRY and NPIIY domains control the timing of germ cell exit from the midgut primordium

To determine how the NRY and NPIIY domain mutants interfere with normal germ cell migration, we used two-photon live imaging to assess the early stages of active migration. By stage 10 in wild-type embryos, cells of the midgut primordium undergo

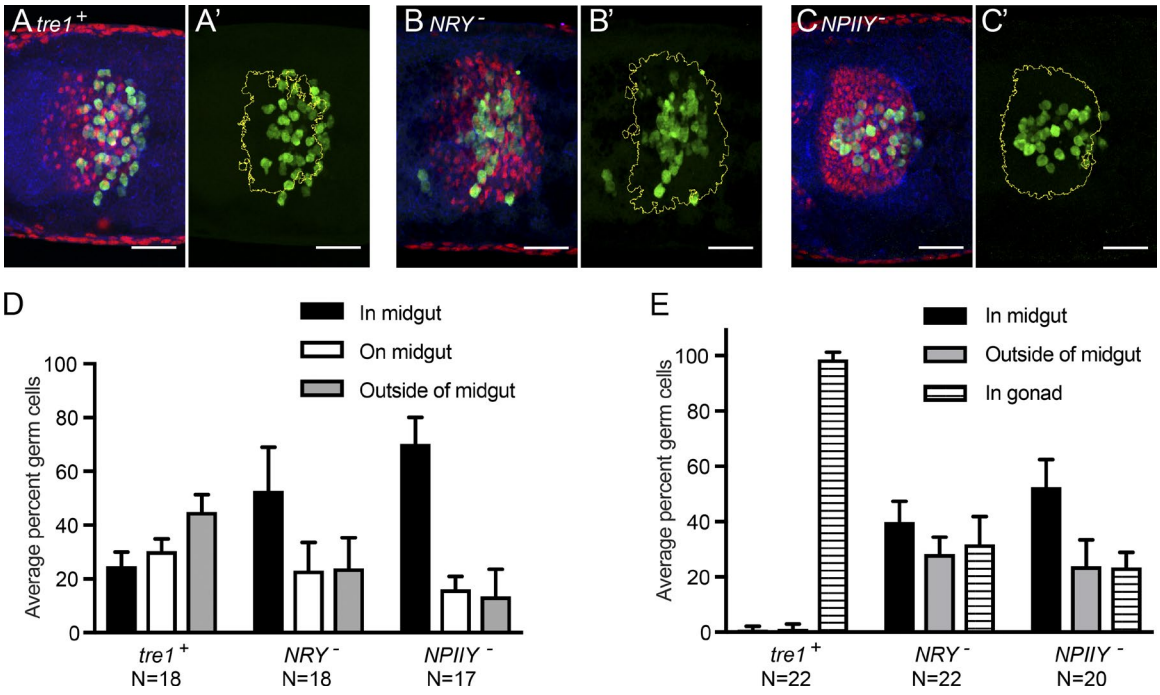

Figure 2. **Both NRY and NPIIY domains are required for proper midgut exit timing.** (A–C) Representative images of fixed embryos at stage 10 stained for Vasa (green, germ cells), Hindsight (midgut, red), and actin (phalloidin, blue). All embryos shown lack maternal and zygotic contribution of endogenous *tre1* gene and inherited maternally provided Tre1 wild-type (*tre1*$^{+}$; A) or mutated forms of the receptor expressed from the respective *tre1* transgene under *nanos* promoter, *nanos* 5′ and 3′ UTRs (B and C). (A′–C′) Outline of the midgut was generated using fluorescent maximum projection of Hindsight staining of midgut nuclei and phalloidin staining of cell cortices. The resulting mask (in yellow) outlines the extent of the midgut primordium. (A) In *tre1*$^{+}$, germ cells exit at stage 10 as the midgut (red) begins delaminating (A′). (B and C) In absence of either domain, germ cells remain in the midgut even after the midgut has undergone epithelial-to-mesenchymal transition (B′ and C′). (D) Bars represent mean percentage of germ cells in each location at stage 10. (E) Bars represent average percent of germ cells in the given location at stage 13 or later. Error bars are standard deviation. Position of germ cells was determined relative to midgut and somatic gonad. At least 17 embryos were analyzed per stage and genotype. N indicates number of embryos analyzed. Bars, 20 µm. For crossing schemes and genotypes, see Table S1.

dynamic changes and begin losing their apical-basal polarity. Their subsequent delamination creates openings through which germ cells cross the primordium (Fig. 2, A and A′; Campos-Ortega and Hartenstein, 1985; Seifert and Lehmann, 2012; Parés and Ricardo, 2016). In both mutants, germ cells exit the midgut primordium later than their wild-type counterpart and follow abnormal migration patterns (Fig. 2, B, B′, C, and C′; Videos 1, 2, and 3; and Fig. S2, A–C). This effect is germ cell–dependent, as midgut polarity and epithelial-to-mesenchymal transition are not affected in *tre1* mutants (Seifert and Lehmann, 2012). Previous studies indicated that late exit from the midgut primordium could cause cells to miss time-sensitive cues (Broihier et al., 1998). In *NRY* or *NPIIY* mutants, germ cells remained associated within the midgut primordium even after the midgut cells started epithelial-to-mesenchymal transition and moved out of the midgut pocket only in late stage 10 (Fig. 2, B–D). By stage 13, when wild-type germ cells have reached the gonad, many germ cells in either *tre1* mutant remained in the midgut or outside the midgut, failing to reach the gonad (Fig. 1, D–F; and Fig. 2 E).

Tre1 NPIIY is required for germ cell polarization

Closer examination of migratory behavior revealed long and persistent extensions at the lagging edge of *tre1* NPIIY mutant germ cells, which were not observed in wild-type controls or NRY mutants (Videos 1, 2, and 3; and Fig. S2, C and D). Because previous studies had shown that before migration, wild-type germ cells polarize by redistributing Rho1, Gβ, and E-cadherin from a uniform distribution along the cell cortex to an enriched concentration at the lagging tail (Kunwar et al., 2008), we wondered whether these abnormal extensions could correlate with alterations in this early polarization step. We confirmed previous immunohistochemical analysis of fixed germ cells containing the *tre1* wild-type transgene, revealing a *tre1*-dependent Rho1 and E-cadherin relocalization (Fig. 3, A and B; and Fig. S3 A). To quantify this redistribution, we compared the concentration of Rho1 on the germ cell cortex normalized to the intensity of Rho1 at the midgut epithelium, as previously described (Kunwar et al., 2008; Fig. 3, E and F). Germ cells with mutations in the NRY domain polarized Rho1 similarly to wild type (Fig. 3, C and F). However, mutating the NPIIY domain caused germ cells to retain higher levels of Rho1 along the germ cell cortices, similar to the phenotype of *tre1*-null mutants (Fig. 3, B, F, and D). In a second quantification method, we measured polarization directly by integrating Rho1 signal intensity across the germ cell cluster averaged among multiple embryos of the same genotype (Fig. 3 G). Both quantification methods demonstrated robust changes in Rho1 cortical distribution and polarization when we compared wild-type germ cells with *tre1*-null mutants (Fig. 3, F and H). They also revealed a wild-type pattern of Rho1 polarization in NRY domain mutant germ cells, whereas Tre1 NPIIY domain mutants failed to localize Rho1, akin to *tre1*-null mutants (Fig. 3, F and H). Previous studies showed that Rho1, E-cadherin, and Gβ localize coordinately to the tail in the wild type (Kunwar et al.,

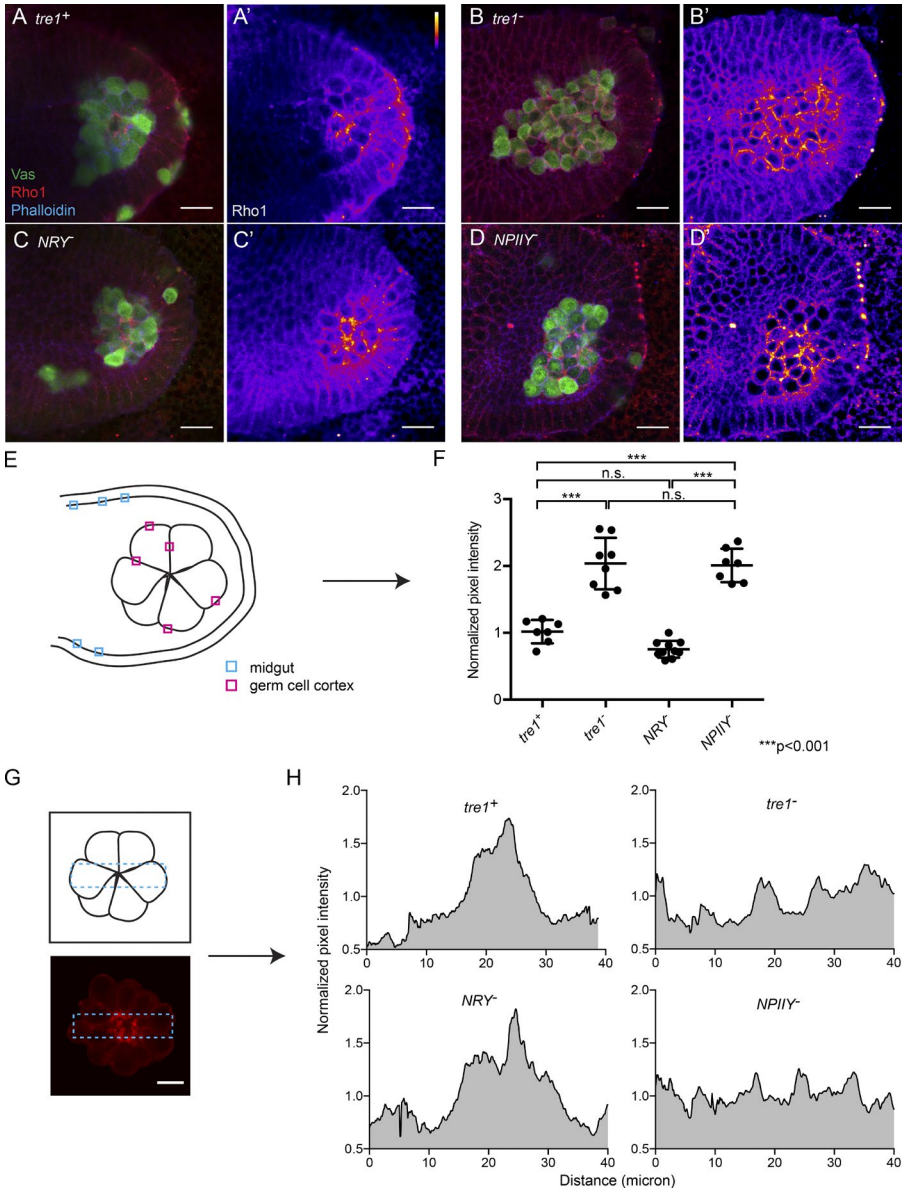

Figure 3. **NPIIY domain, but not NRY domain, is required for Rho1 localization and germ cell polarization.** (A–D) Representative images of embryos at stage 9 stained for Vasa (green, germ cells), Rho1 (red), and actin (phalloidin, blue). Bar, 20 µm. All embryos shown lack maternal and zygotic contribution of endogenous *tre1* gene. Embryos in A, C, and D inherited maternally provided Tre1 wild-type (*tre1*$^{+}$; A) or mutated forms of the receptor *NRY*$^{-}$ (C) and *NPIIY*$^{-}$ (D) expressed from the respective *tre1* transgene under *nanos* promoter, *nanos 5′* and *3′* UTRs. (A′–D′) Rho1 intensity measurement portrayed in fire pseudocolor from black/blue (low) to yellow/white (highest). Rho1 concentrates in tail region and germ cells polarize in embryos with Tre1^{+} and Tre1 NRY^{-} receptors. Polarity is lost, and Rho1 distributes along germ cell cortex in embryos lacking Tre1 (B) or Tre1 NPIIY^{-} (D) mutant receptor. Bars, 20 µm. For crossing schemes and genotypes, see Table S1. (E–H) Quantification of cortical concentration and polarization. (E) To measure cortical concentration of Rho1, intensities of at least five ROIs; 72 pixels each) of germ cell cortices (pink) were measured using ImageJ and compared with anterior midgut cortices (blue) as internal controls. Intensity of averaged germ cell ROI measurements was normalized to averaged midgut ROI measurements (Kunwar et al., 2008). (F) Localization quantification is graphed using a minimum of seven embryos for each maternal genotype described in A–D. Relation of germ cell cortex/midgut cortex measurement of wild type was arbitrarily set to 1. ***, P < 0.0001. Error bars represent standard deviation. (G) Polarization quantification. The fluorescent intensity of a 10-µm, one germ cell diameter rectangle encompassing the entire width of the germ cell cluster (35–55 µm) was measured. Fluorescent intensities were normalized to the mean intensity from each embryo and plotted. Bar, 10 µm. (H) At least five embryos for each maternal genotype described in A–D were measured and the intensities aligned to the center.

2008; LeBlanc, 2016). In agreement, we observed E-cadherin localization affected by NPIIY mutants but not NRY mutants (Fig. S3 A). Thus, the NPIIY domain is specifically required for the initial germ cell polarization. We propose that loss of polarity may cause prolonged adhesion and a failure of germ cells to properly extend and retract filopodia. These defects may account for the delayed exit from the midgut observed during live imaging of NPIIY mutants.

Tre1 NRY domain is required for recognition of midline cues

We next asked whether Tre1 signaling via the NRY or NPIIY domain affected the germ cell guidance function. Wild-type germ cells sort bilaterally after exiting the midgut to evenly occupy the laterally positioned gonads (Sano et al., 2005; Renault et al., 2010). Bilateral sorting is achieved through Wunen LPP-dependent repulsion. Because of high somatic expression of Wunen, germ cells do not cross the ventral midline and avoid the ectoderm (Sano et al., 2005). We noted that in *tre1*^{sctt} embryos, which carry a deletion of the NRY domain, germ cells migrated into the epithelium, which they normally avoid. The same aberrant migration phenotype was also observed in the NRY domain mutant, but not the NPIIY domain mutant (Video 2 and Fig. S2, B–D). This phenotype has previously been seen only in embryos that lack *wunen* in the soma (Mukherjee et al., 2013). To address a potential relationship between Tre1 and Wunen, we focused on the hallmark feature displayed by mutants that lack Wunen guidance cues in the soma: bilateral sorting. Whereas wild-type germ cells sort bilaterally after exiting the midgut and avoid the ventral midline, germ cells in *wun/wun2* zygotic mutant embryos, which lack Wunen in all somatic tissues, cross the midline (Sano et al., 2005). To better quantify this step in germ cell migration and circumvent the need for live tracing and reconstruction of individual germ cell trajectories within wild-type and mutant embryos, we adapted a recently developed photoactivation assay (Slaidina and Lehmann, 2017). We expressed a photoactivatable GFP (PAGFP) throughout the early embryo (Patterson and Lippincott-Schwartz, 2002; Murray and Saint, 2007). GFP was photoactivated in one to three germ cells in stage 5 embryos, just after germ cell formation. All

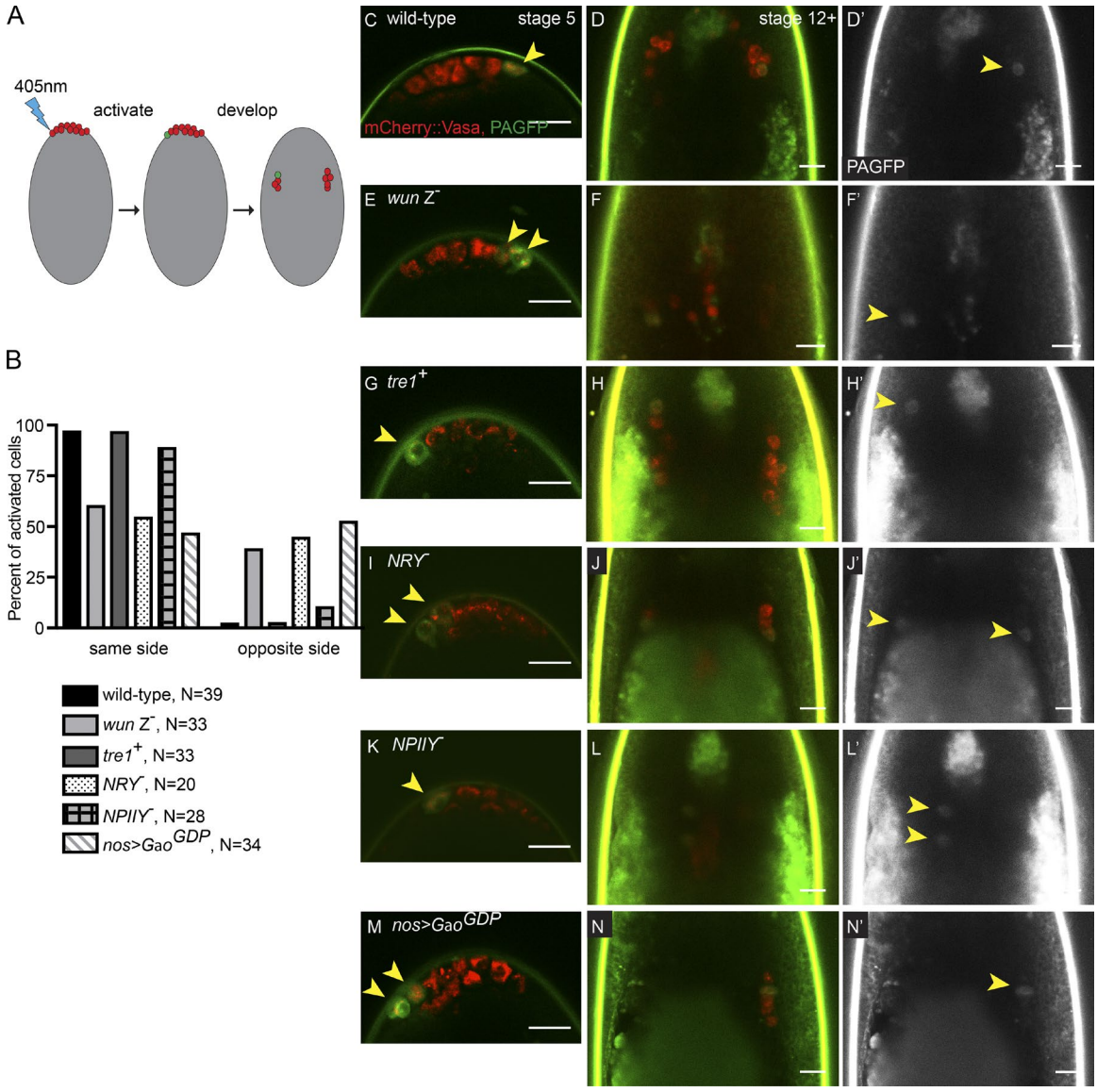

Figure 4. **NRY domain, but not NPIIY domain, is required for germ cell bilateral sorting.** (A) Experimental design. Embryos carrying the mCherry::Vasa fusion protein, which marks all germ cells (red), as well as the *nanosGal4*::VP16 driving UAS-αTub::photoactivatable GFP (PAGFP), were oriented dorsal side down on a coverslip and activated with a 405-nm laser laterally just after germ cell formation at the posterior pole (stage 5) and allowed to develop until germ cells had laterally sorted and entered the mesoderm (stage 12 or later). (B) Quantification of photoactivated germ cells of the indicated genotype that followed midline cues and migrated to the same side gonad with respect to their formation ("same side") or moved to opposite sides ("opposite side"). N represents the number of activated germ cells analyzed. Data are summarized in Table S3; for crossing schemes and genotypes, see Table S1. Wild-type embryos (C) and embryos lacking *wun* and *wun 2* zygotically (*wun* Z⁻; E) were used as controls for germ cells responding and unresponsive to midline cues, respectively. (C, E, G, I, K, and M) Representative images of germ cells with PAGFP (green) in lateral germ cells at stage 5 in embryos of indicated genotypes. (D, F, H, J, L, and N) Visualization of the same photoactivated cells in embryo of respective genotypes. Activated cells are denoted with yellow arrows in D′, F′, H′, J′, L′, and N′. Bars, 20 µm.

germ cells were visualized by Vasa fused to mCherry (Lerit and Gavis, 2011). Embryos were mounted on their ventral surface, and germ cells on the lateral most edge (left or right) were photoactivated (Fig. 4 A). We determined which side of the embryo the photoactivated germ cells occupied at stage 12 of embryogenesis, when germ cells normally have associated with the somatic gonad, and correlated this with the site of photoactivation at stage 5. Wild-type germ cells robustly retained their lateral position (left or right) relative to the developing embryo, with <10% of germ cells crossing the midline between the time of formation and their homing to the gonad (97.4% of photoactivated cells avoided the midline, $n = 39$; Fig. 4, B–D).

To further evaluate our method, we asked whether we could recapitulate previous results demonstrating defects in bilateral sorting in *wun/wun2* mutant embryos (Sano et al., 2005). Indeed, photoactivated germ cells in the zygotic *wun/wun2* mutant background failed to sort along the midline, only 60% of germ cells remained on the same side of the embryo when photoactivated at stage 5 and scored at stage 12, suggesting random migration (60.6% avoided the midline, $n = 33$; Fig. 4, B, E, and F). These findings establish photoactivation as a reliable and efficient method to observe midline sorting and confirm previous observations that Wunen LPPs are required for producing guidance cues that repel germ cells. Further, this assay

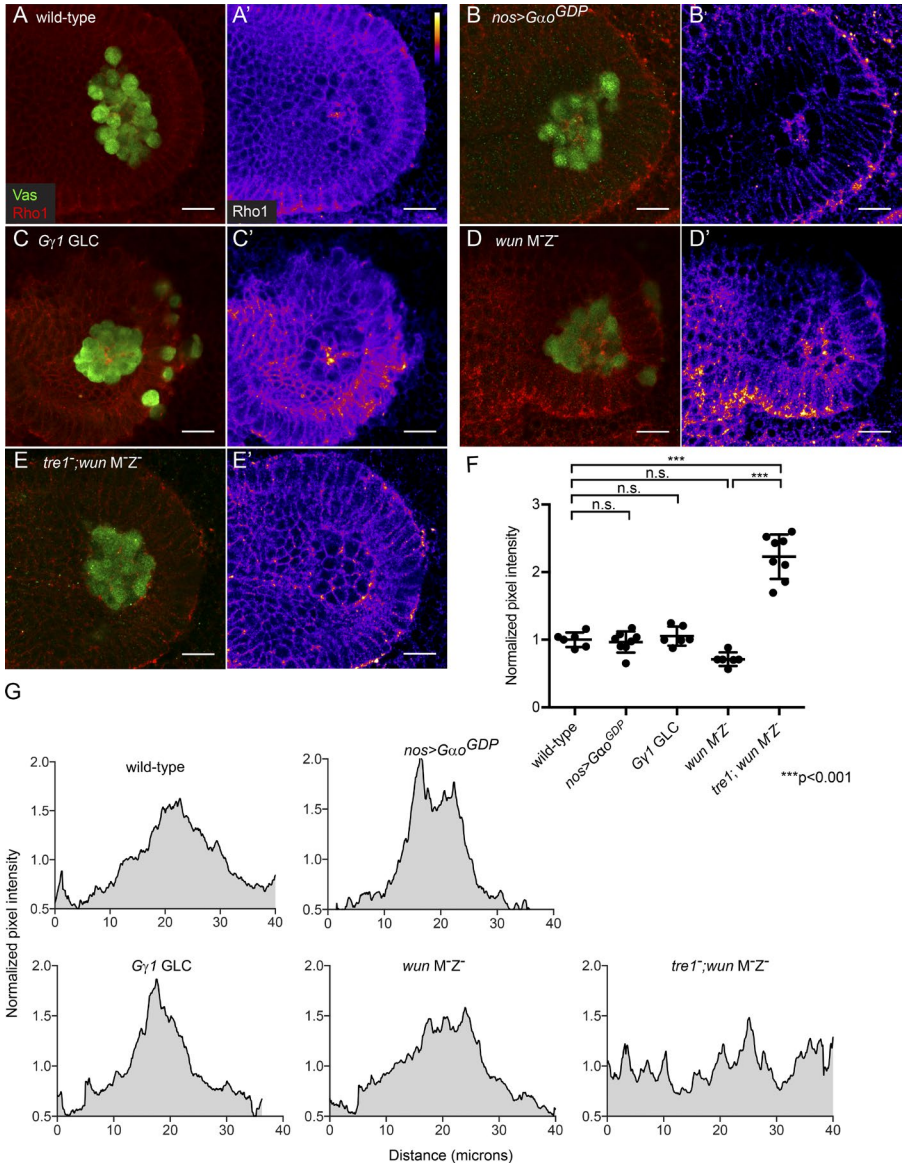

Figure 5. **Wunen and G protein signaling are not required for germ cell polarization.** (A–E) Representative images of embryos at stage 9 stained for Vasa (green, germ cells), Rho1 (red), and actin (phalloidin, blue). Bars, 20 µm. Rho1 concentrates in tail region, and germ cells polarize in wild-type embryo and embryos in which G protein signaling was blocked (A), either by overexpression of Gαo GDP (B) or by removal of Gγ1 from germ cells (C). (D) In the absence of germ cell and somatic *wunen* (*wun* $M^{-}Z^{-}$), germ cells localize Rho1 and polarize similar to wild-type germ cells. (E) Polarization and Rho1 localization fail in absence of both *wunen* and *tre1*. (A′–E′) Rho1 intensity measurement portrayed in fire pseudocolor from black/blue (low) to yellow/white (highest). (C) Gγ1 GLCs (germline clone) require rescue in the somatic tissue (see Materials and methods) to allow for gastrulation. This rescue is not complete, as evident by abnormal posterior midgut morphology seen in many embryos. Germ cells, nonetheless, are still able to polarize (F and G). (F) Quantification of cortical Rho1 concentration graphed as per Fig. 3 E. Error bars represent standard deviation. (G) Polarization quantifications as in Fig. 3 G. For crossing schemes and genotypes, see Table S1.

revealed that the position of germ cells at the time of specification is retained through internalization and transepithelial movements of germ cells.

To test whether *tre1* domain mutants were able to recognize and respond to Wunen guidance cues, we photoactivated individual germ cells and assessed midline repulsion. The *tre1*$^{+}$ transgene fully rescued the *tre1* mutant phenotype, and germ cells followed midline guidance similar to the wild-type control (97% of photoactivated cells avoided the midline, $n = 33$; Fig. 4, B, G, and H). Mutations in the NRY domain resulted in germ cells migrating at random, regardless of the original position of the germ cells, similar to *wun/wun2* zygotic mutants (55% avoided the midline, $n = 20$; Fig. 4, B, I, and J). Germ cells that inherited a mutant NPIIY domain protein, however, migrated toward the gonad according to their position at germ cell formation (89.3% avoided the midline, $n = 28$; Fig. 4, B, K, and L). This suggests that the NRY domain but not the NPI IY domain of Tre1 is required for receiving and/or responding to Wunen migration cues.

Studies in other systems suggest the NRY domain functions as a scaffold for the G protein complex. In neuroblasts, Tre1 was shown to signal through Gαo to orient their division axis in relation to the embryonic epithelium (Yoshiura et al., 2012). To deplete Gαo activity in germ cells while avoiding patterning defects during oogenesis and embryogenesis, we expressed a dominant-negative GDP-bound form of Gαo (*Gαo*^{GDP}) specifically in PGCs using the germline-localized *nosGal4* driver (see Table S1). Overexpression of this construct caused strong migration defects, with only 48% of germ cells reaching the gonad (48.3 ± 2.1%, $n = 39$; Fig. S3 C), and affected lateral sorting (47.1% avoiding the midline, $n = 34$; Fig. 4, B, M, and N), similar to the NRY mutants. These experiments suggest that Tre1 NRY domain acts via Gαo and that this interaction is necessary for proper recognition of midline cues provided by Wunen.

Rho1 localization is independent of G protein signaling and Wunen LPP

Our results suggest that the NRY domain of Tre1 mediates Wunen-dependent germ cell repulsion through G protein signaling. This function is specific to the NRY domain and does not require the NPIIY domain of Tre1. We therefore asked

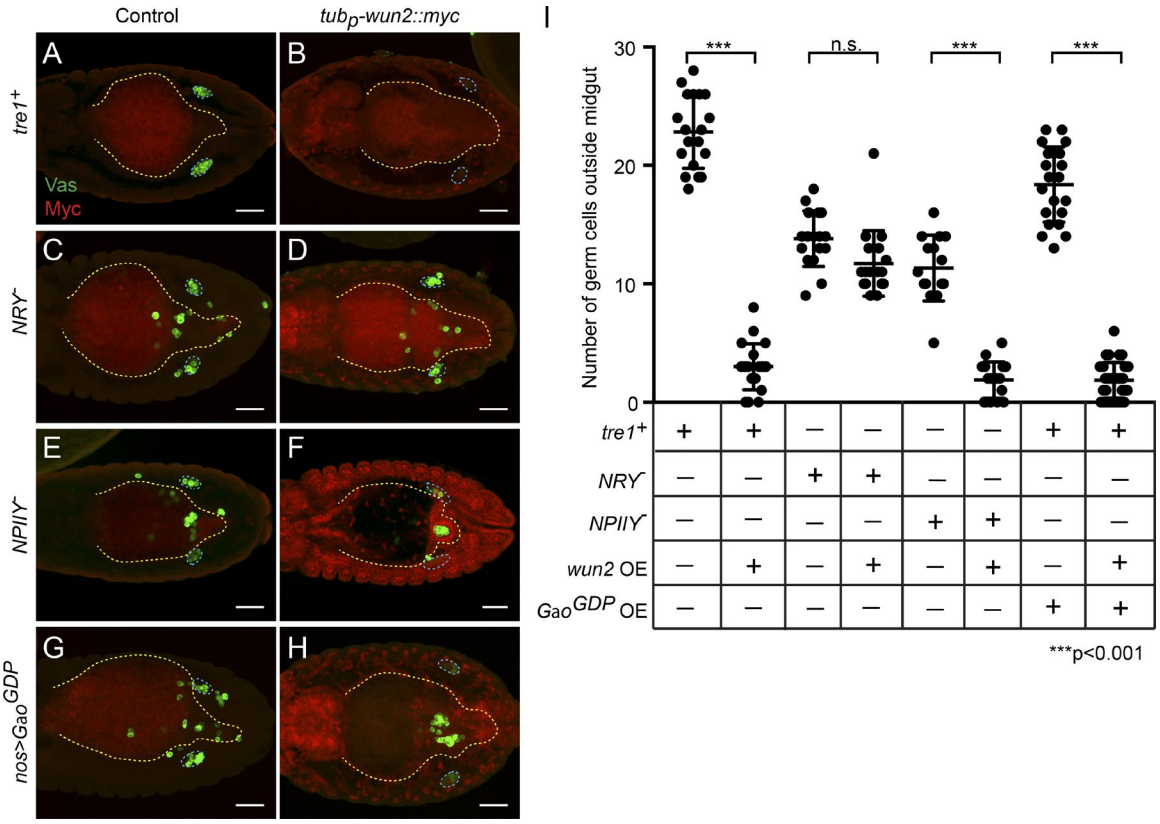

Figure 6. **Tre1 NRY domain is required for response to Wunen-mediated death.** (A) *tre1*+ embryos average with ~24 germ cells in the gonads by stage 12 or later. (B) Overexpression of Wunen in the soma (*tub$_P$-wun2::myc* written as *wun2* OE, red) results in massive germ cell death. (C–G) Germ cells with NRY (C) or NPIIY (E) mutant Tre1 receptors or germ cells (G) expressing the dominant-negative form of Gαo remain in the midgut or scatter in the embryo. (D) Overexpression of somatic *wunen* does not alter the *NRY* mutant phenotype. (F) Overexpression of somatic *wunen* in NPIIY embryos kills the majority of germ cells that exit the midgut. (H) Overexpression of *wunen* in embryo expressing Gαo dominant-negative form in germ cells kills the majority of germ cells. All embryos are viewed from dorsal. The midgut is outlined in yellow hashes and the gonad in white hashes to distinguish between different germ cell populations. (I) Quantification of number of germ cells is shown for germ cells outside the midgut, as they are susceptible to Wunen-mediated germ cell death. For total number of germ cells see Fig. S4 C. Bar, 50 µm. ***, P < 0.001. Error bars represent standard deviation. For crossing schemes and genotypes, see Table S1.

whether the initial polarization event, which seems specifically mediated by the NPIIY domain, required G proteins or Wunen. As described above, we disrupted Gαo signaling by expressing Gαo^{GDP} specifically in PGCs. Analysis of Rho1 and E-cadherin distribution revealed that Gαo signaling is apparently dispensable for redistribution and thus PGC polarization (Fig. 5, A, B, F, and G). Next we disrupted Gγ by generating Gγ1 mutant germline clones and restoring embryonic patterning by expressing *Gγ1* specifically in somatic cells (described by Kunwar et al., 2008). As previously shown, Gγ1 acts downstream of Tre1 GPCR and produces a strong germ cell migration defect, with the majority of germ cells failing to exit the midgut. Like *Gαo^{GDP}*, Rho1 polarized normally in *Gγ1* mutant germ cells (Fig. 5, C, F, and G). Collectively, these results strongly suggest that the NPIIY domain of Tre1 promotes germ cell polarization independently of G protein signaling. We next asked whether Wunen activity played a role in PGC polarization. Rho1 and E-cadherin were properly redistributed to the germ cell tail in *wun* M$^-$Z$^-$ mutants (Fig. 5, D, F, and G; and Fig. S3 A). However, mutating *tre1* in *wun M$^-$Z$^-$* mutant background affected Rho1 polarization similar to loss of Tre1 alone (Fig. 3 B and Fig. 5, E–G). These results argue that the function of Tre1 in PGC polarization is independent of G protein and Wunen activity.

NRY domain responds to Wunen-dependent survival cues

Germ cell survival is intricately linked to Wunen function. Loss of *wun2* in germ cells or overexpression of *wun*/*wun2* in somatic tissues, leads to extensive germ cell death (Fig. S4 A). This death is observed only after germ cells have traversed the midgut primordium (Starz-Gaiano et al., 2001; Hanyu-Nakamura et al., 2004; Renault et al., 2004, 2010). Because Wunen functions as an LPP, these results have been interpreted as an indication for a competition between Wunen expressed in somatic tissues, which depletes the lipid phosphate pool from the environment, and germ cell–expressed Wun2, which uses hydrolysis of the lipid phosphate for germ cell survival (Renault et al., 2004). This model suggests that normally germ cells and soma strike a balance of phospholipid hydrolysis and lipid uptake. This balance is shifted by removing *wun2* from germ cells or by overexpressing *wunen* in somatic tissues, resulting in extensive germ cell death (Fig. 6, A and B; Renault et al., 2004). Previously it had been shown using a *tre1*-null mutation that germ cell death upon *wunen* overexpression was blocked (Renault et al., 2010). However, because midgut exit is blocked in *tre1*-null mutants, the relationship between Tre1 and Wunen could not be assessed in this experimental setting (Renault et al., 2010). Therefore, we took advantage of the *tre1^{sctt}* hypomorphic allele and the

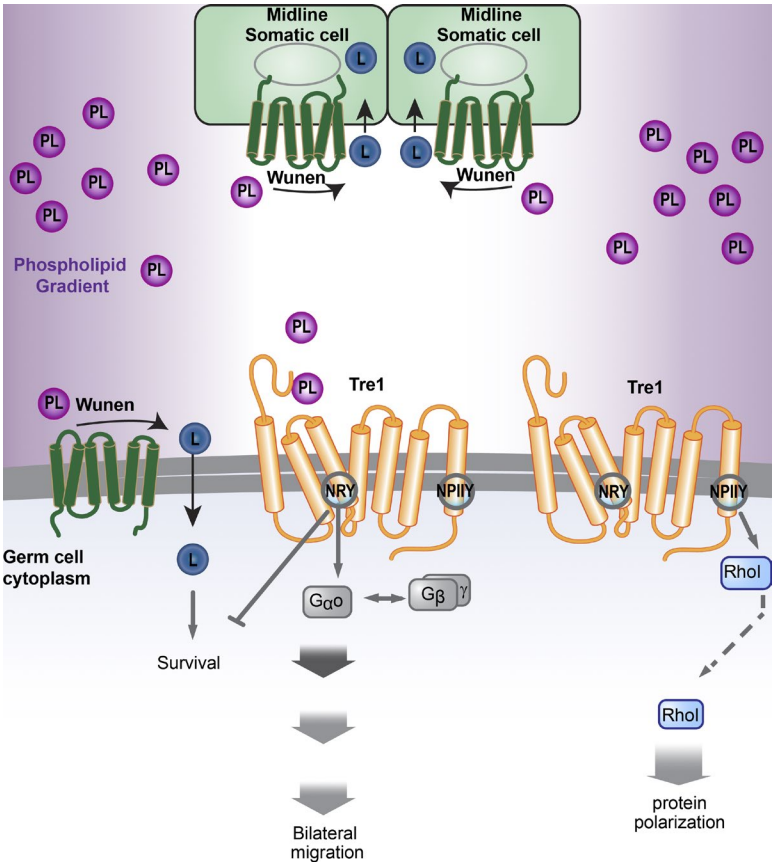

Figure 7. **Tre1 multifunctional domain model.** Germ cells express both Wunen (green) and Tre1 (orange). We hypothesize that a still unknown phospholipid (PL) acts as a ligand for Tre1. This putative Tre1 ligand is distributed along gradients generated in somatic tissues via Wunen-dependent PL hydrolysis and lipid uptake. Germ cells move toward higher concentrations of the PL and, as a consequence, away from Wunen-expressing tissues. Expression of Wunen in the neuroectoderm leads to bilateral sorting of germ cells away from the ventral midline (top). Activation of the receptor and bilateral sorting requires the NRY domain and is mediated by Gαo signaling. The NPIIY domain of Tre1 acts via Rho1, possibly mediated by receptor dimerization. This leads to cell polarization and redistribution of Rho1 and E-cadherin to the germ cell tail. Wunen expression in germ cells promotes germ cell survival. This Wunen-dependent survival function is somehow counteracted by Tre1. This function of Tre1 is mediated by the NRY domain but is independent of Gαo signaling.

NRY and NPIIY domain mutants, in which some germ cells migrate out of the midgut and thus should become sensitive to lipid-phosphate survival signals. Surprisingly, *tre1*^{scrt} mutant germ cells survive even after removing *wun2* from germ cells or after overexpression of Wunen in somatic tissues, genetic backgrounds that result in germ cell death in a *tre1* wild-type background (Fig. S4 B; Hanyu-Nakamura et al., 2004; Renault et al., 2004). To assess the relative contributions of the NRY and NPIIY domains, we increased somatic Wunen levels in either NRY or NPIIY mutants. Because germ cells respond to Wunen-mediated death only when they exit the protective midgut environment, we compared the number of germ cells outside the midgut as well as the total number of germ cells (Fig. 6 I and Fig. S4, B and C). In wild-type control, *tre1*$^{+}$ embryos, overexpressing Wun in the soma results in germ cell death upon midgut exit, leaving one sixth of the normal number of germ cells in the gonad (22.8 ± 3.1 germ cells, n = 23 normally, and 3.1 ± 1.7 germ cells, n = 21 upon Wun overexpression; Fig. 6, A, B, and I). In contrast, we found Wun overexpression in embryos carrying the *tre1 NRY* mutant caused germ cells to survive outside the midgut similar to sibling control in which Wun is not overexpressed (13.8 ± 2.4 germ cells, n = 18, and 11.7 ± 2.8 germ cells, n = 18, respectively; Fig. 5, C, D, and I). Germ cells in a *tre1 NPIIY* mutant background, however, displayed *wunen*-dependent cell death, with few to no germ cells surviving outside the midgut (1.9 ± 1.5 germ cells, n = 17, and 11.3 ± 2.8 germ cells, n = 15, in control siblings) and significantly fewer germ cells surviving overall (Fig. 5, E, F, and I; and Fig. S4 C). These results suggest that the NRY but not the NPIIY domain of Tre1 interferes with Wunen-dependent germ cell survival cues. Germ cells expressing dominant-negative Gαo were susceptible to Wunen-mediated death (1.9 ± 1.5 germ cells, n = 36, vs. 18.7 3.2 germ cells, n = 21, in sibling control), suggesting that this function of the NRY domain is not mediated by G protein signaling (Fig. 6, G–I; and Fig. S4 C).

Discussion

Here we provide genetic and functional evidence that the Tre1 GPCR engages separate signaling pathways to mediate distinct migratory behaviors. We show that two highly conserved protein domains within the Tre1 GPCR, the NPIIY and the NRY motifs, cooperate in the overall ability of germ cells to engage in migration but also mediate distinct and separable roles in germ cell migration and survival. The NPIIY motif in TM7 polarizes germ cells at the onset of migration, while the NRY motif in TM3 plays a role in responding to directional migration and survival cues (Fig. 7). Our findings support a direct link between Tre1 GPCR function and lipid phosphate signaling.

Live imaging suggests that NPIIY-dependent Tre1 signaling modulates the actin cytoskeleton at the onset of their migration. We show that the NPIIY domain is specifically required for the reorganization of Rho1 and E-cadherin in germ cells to allow individualization of germ cells and distinct leading edge–lagging edge polarity. In the absence of NPIIY function, germ cells form long extensions, and migration is delayed. Previous studies have shown that the NPxxY domain can mediate ligand-independent receptor internalization (Kalatskaya et al., 2004), and recent molecular dynamics experiments on the adenosine A2A receptor, the β2-adrenergic receptor, and rhodopsin have suggested that the NPxxY motif mediates formation of a

continuous water channel in the active state (Yuan et al., 2014). This active confirmation is stabilized by an interaction between the tyrosine residue in the NPxxY motif and the DRY domain (Yuan et al., 2014). Although we did not directly test for the function of the tyrosine residue in the NPIIY motif of Tre1, our finding that mutations in the NRY and NPIIY domains result in different phenotypes suggests independent pathways. Our findings are more consistent with studies in mammalian tissue culture in which RhoA (Rho1 in *Drosophila*) was shown to form a functional complex with GPCRs that contain an NPxxY but not a DPxxY motif. The authors observed that RhoA-GPCR interaction elicited an increase in phospholipase D activation independent of the "classical" heterotrimeric G protein signaling pathway (Mitchell et al., 1998; Borroto-Escuela et al., 2011). Accordingly, we propose that upon receptor activation, Rho1 activation and binding to Tre1 GPCR through the NPIIY motif recruits E-cadherin. Subsequent relocalization of Rho1 and E-cadherin would result in individualization of germ cells and cell polarization. A mechanism by which a single GPCR can activate separate signaling pathways has been recently proposed for the chemokine receptor CCR7. Hauser et al. (2016) showed that inflammatory signals induce dimerization of CCR7 in migratory T and dendritic cells. CCR7 elicits the classical heterotrimeric G protein signaling pathway and, upon receptor oligomerization, a second pathway dependent on Src binding and phosphorylation. Intriguingly, receptor oligomerization requires a hydrophobic interaction surface near the NPxxY domain of CCR7. Parallel signaling in CCR7 makes immune cell migration more efficient (Hauser et al., 2016). Facultative receptor dimerization creating an interaction surface for Rho1 is one mechanism that could explain how in germ cells the single Tre1 receptor can provoke distinct migratory responses (Fig. 7). We do not know how the NPIIY domain is regulated. One intriguing possibility is that reorganization of E-cadherin in the underlying midgut epithelium may provide a cue for germ cell polarization (Parés and Ricardo, 2016).

In contrast to the NPIIY domain, we show that the NRY domain of Tre1 is dispensable for germ cell polarization but instead is required for dispersal, directional migration, and germ cell survival. In many Rhodopsin-like receptors, E/N/DRY domains play important roles in heterotrimeric G protein activation upon ligand binding (Zhu et al., 1994; Acharya and Karnik, 1996; Scheer et al., 1996; Rasmussen et al., 2011). As previously shown for neuroblast polarization, we find Gαo is also required downstream of Tre1 for germ cell migration (Yoshiura et al., 2012). Combined, these data imply that the Tre1 NRY domain is required for responding to migration cues that induce G protein activation and result in proper migration (Fig. 7).

Our results suggest a connection between the Tre1 NRY domain and Wunen-dependent lipid phosphate signaling (Fig. 7). One possibility is that a Wunen-regulated phospholipid is the still evasive Tre1 ligand. Alternatively, phospholipids could allosterically regulate Tre1 activity, as has been shown for β2-adrenergic receptor in regulating GPCR activity (Dawaliby et al., 2016). In support of a phoshopholipid being the Tre1 ligand, the human Tre1 homologue, GPR84, binds medium chain fatty acids, and D-Cerk and D-Mulk, two *Drosophila* ceramide kinase homologues, have been shown to mediate PGC migration (Wang et al., 2006; McElwain et al., 2011). The mammalian homologue of Wunen, LPP3, regulates sphingosine-1-phosphate (S1P) levels and controls the circulation of T cells in the mouse and allows for their thymic egress (Bréart et al., 2011). In vertebrates, S1P and lysophosphatidic acid are ligands for dedicated S1P and lysophosphatidic acid GPCRs, and several of these have been implicated in regulating migratory behavior in immune cells, cardiomyocytes, and metastatic carcinoma cells (Mendelson et al., 2014; Baeyens et al., 2015). Germ cell migration in vertebrates, however, is largely governed by the chemokine CXCL12/SDF1 and its receptor CXCR4 (Doitsidou et al., 2002; Ara et al., 2003; Knaut et al., 2003; Molyneaux et al., 2003). Recent data in zebrafish suggest that in addition, repulsive cues are mediated by zebrafish LPPs/Wunens and that these cues are needed for germ cells to settle in the gonad region (Paksa et al., 2016). In the ascidian *Botryllus schlosseri*, S1P signaling has been implicated in germ cell guidance, and *Botryllus* germ cells express S1P receptors (Kassmer et al., 2015). In vertebrate germ cells and immune cells, the CXCR4 chemokine and S1P phospholipid receptors appear to mediate distinct behaviors of migratory cells. Our data suggest that in *Drosophila*, a single GPCR mediates two distinct downstream migratory behaviors, suggesting a functional connection between chemokine and phospholipid recognition.

Our results also show that mutations in the DRY domain protect germ cells from death. This surprising role for Tre1 is apparent only when germ cell survival is challenged, either by lack of Wunen in germ cells or overexpression of Wunen in the soma. It is possible that phospholipid binding to the receptor somehow deprives germ cells of a lipid source and that in the DRY mutant, this source is now available for PGC survival. Although we do not know how Tre1 affects PGC survival, our data strongly suggest a primary role for germ cell–expressed Wunen in survival rather than migration. Indeed, a role for Tre1 as a dedicated phospholipid receptor in germ cells can explain why PGCs that lack Wun2, but have normal Wunen expression in the soma, die in large numbers but can still follow migratory cues and properly reach the gonad (Hanyu-Nakamura et al., 2004).

Collectively, our results reveal two genetically separable downstream pathways of a single GPCR in germ cell migration. Our data suggest that Tre1 via G protein signaling is responsible for directed germ cell migration by reading a phospholipid gradient generated by Wunen lipase activity, while PGC polarization occurs separate from ligand-dependent G protein activation, either by a second ligand or by ligand-independent mechanisms. This type of dual signaling could be akin to Src activation upon CCR7 dimerization, which is independent of the classical G protein signaling pathway but requires receptor conformation changes because of receptor dimerization (Hauser et al., 2016). Combining separate controls for directed migration and polarity in a single receptor not only makes the process more robust but also provides opportunity for distinct spatial and temporal regulation to the migration process.

Materials and methods

Fly stocks

Animals were raised in polystyrene vials containing a medium of yeast, molasses, and cornmeal and kept at 25°C, unless otherwise indicated. Stocks used in this study include the following: w^{1118} as a wild-type control, $tre1^{\Delta EP5}$ is a deletion of the first exon of CG3171 and behaves as a null mutation for Tre1 (Ueno et al., 2001; Kunwar et al., 2003), and $tre1^{sct}$ is a single-nucleotide mutation in $tre1^{sctt}$, which changes the splice acceptor site of the fourth intron. This causes a 24-bp deletion from exon 5, resulting in a seven amino acid deletion, including the "RY" of the "NRY"

motif. Further analysis revealed that an alanine, "AY" substitution recapitulates the *tre1*^{sctt} phenotype (Coffman et al., 2002; Kamps et al., 2010), *nosmoesin::GFP* (Sano et al., 2005), *nosGal4*::VP16 (Van Doren et al., 1998), *tub*$_p$*-wun2*::myc (Renault et al., 2004), *UASp-*α*tub::PAGFP* (Murray and Saint, 2007), *mCherry-vasa* (Lerit and Gavis, 2011), *wun2*^{N14} (Hanyu-Nakamura et al., 2004), *Df(2R)w45-19g* (Hanyu-Nakamura et al., 2004), *wun*^{ex49}*wun2*^{ex34} (Renault et al., 2010), *Gγ1*^{N159} (Izumi et al., 2004), *UAS-Gαo*^{GDP} UAS-*Gαo*^{GTP} (both Gαo stocks were gifts from A. Tomlinson, Columbia University Medical Center, New York, NY; Katanaev et al., 2005), and *nulloGal4* (Kunwar et al., 2003). *w*^{1118} and *ovoD* FRT lines (for Gγ1 germline clone generation) were obtained from the Bloomington Drosophila Stock Center collection. Lines generated for this study include *nos*$_p$*-tre1*$^+$ *flag*, *nos*$_p$*-tre1 NRY*$^-$ *flag*, *nos*$_p$*-tre1 NPIIY*$^-$ *flag*, *nos*$_p$*-tre1 NRY*$^-$*NPIIY*$^-$ *flag*, and *nos*$_p$*-tre1 D266A*. All lines containing the *tre1*$^{\Delta EP5}$-null allele are written as *tre1*$^-$. Throughout the text, we refer to embryos derived from mutant females as "mutant embryos," referring to the maternal genotype.

Because there is a paternal contribution to the *tre1* phenotype due to early zygotic germ cell expression of the *tre1* gene (Coffman et al., 2002), we depleted *tre1* maternal and zygotic sources as indicated in Table S1. *tre1* transgenic constructs use the *nanos* promoter, which is not zygotically active until late stages of embryogenesis. We did not observe any paternal rescue with the *tre1*$^+$ transgene and therefore did not account for the zygotic transmission of the respective *tre1* transgenes. Crossing schemes for each figure are outlined in Table S1.

To generate embryos that lacked maternal *wun* and *wun2*, we used females carrying the dominant-negative *wun2*^{N14} allele (Hanyu-Nakamura et al., 2004; Renault et al., 2010) in trans to the *wun*, *wun2* deficiency *Df(2R)w45-19g*. This genetic combination recapitulates the phenotype of germ line clones homozygous for *wun* and *wun2* null mutations (Hanyu-Nakamura et al., 2004; Renault et al., 2010). To identify *wunen* zygotic (somatic) loss-of-function conditions in Fig. 4 and Fig. S4, genotypically mutant embryos were identified by lack of LacZ, expressed by balancer chromosome, with genotypes as shown in Table S1.

Gγ1 germline clones were generated using the ovoD Flp-FRT technique. Gastrulation defects were rescued by expression of the *Gγ1* gene (UAS-Gγ1) in somatic tissue using the *nulloGal4* driver (Kunwar et al., 2008).

Generation of mutant transgenes

NRY and NPIIY domain mutations were generated in *tre1* cDNA and inserted into vectors with and without a C-terminal Flag and Myc peptide. Germ cell–specific expression was driven by the *nanos* promoter, and translation was restricted to the germ plasm via the *nanos* 3′UTR (Gavis and Lehmann, 1992, 1994; Van Doren et al., 1998). After manipulation, the *tre1-nos3′*UTR cDNA remained unchanged, with the exception of point mutations indicated in Fig. 1 A. The constructs were placed in the Valium 22 *Drosophila* vector for P2 site-specific integration using NdeI and EcoRI digest sites and Gibson cloning technique (Groth et al., 2004; Gibson et al., 2009; Ni et al., 2011). Primer sequences are described in Table S2.

Immunohistochemistry

Embryos were kept at 25°C and collected for 2 h and allowed to age to the appropriate stage. Visual landmarks, such as midgut morphology and degree of head involutions, were used to compare embryos at same stage (Seifert and Lehmann, 2012). The chorion was removed by incubation in 50% bleach for 3 min. Embryos were fixed in 4% methanol-free formaldehyde and heptane and hand devitellinized with 28-gauge 1/2 needles (BD) in PBS with 0.1% Trion X-100 and 1% BSA. Embryos were incubated overnight with primary antibody and then for 2 h with secondary antibody and mounted in VECTASHIELD (H1000; Vector Laboratories) for imaging. To visualize *tre1* transgene protein distribution, stage 5 embryos were cut at the posterior and mounted such that the germ cells were all visible in one focal plane (Slaidina and Lehmann, 2017).

Gγ1 germ line clones required fixation in methanol because of decreased embryo production. Embryos were collected and fixed in 4% formaldehyde and devitellinized with heptane and methanol (Sano et al., 2005). Embryos were then shaken with methanol, rinsed, and kept at −20°C in methanol until enough embryos were pooled for further processing. Embryos from the *wunen* misexpression experiments were also fixed using methanol. Subsequent staining procedure and antibodies were as described above.

The following primary antibodies were used: rabbit anti-Vasa (1:5,000; Lehmann laboratory), mouse anti-Hindsight (1G9; Developmental Studies Hybridoma Bank; 1:50), mouse anti-Eya (eya10H6; Developmental Studies Hybridoma Bank; 1:20), mouse anti-Rho1 (p1D9; Developmental Studies Hybridoma Bank; 1:100), rat anti–DE-cadherin (DCAD2; Developmental Studies Hybridoma Bank; 1:50), mouse anti-Flag (F1804; Sigma-Aldrich; 1:200), and mouse anti-Sxl (M18; Developmental Studies Hybridoma Bank; 1:200). Secondary antibodies used included phalloidin–Alexa Fluor 633 (A22284; Invitrogen; 1:500), Alexa Fluor 555 anti–mouse (A21424; Invitrogen; 1:500), CY3 anti–mouse (715-165-151; Jackson ImmunoResearch Laboratories, Inc.; 1:500), Cy3 anti–rat (712-165-150; Jackson ImmunoResearch Laboratories, Inc.; 1:500), Alexa Fluor 488 anti–rabbit (A11039; Thermo Fisher Scientific; 1:500), and anti-myc Alexa Fluor 555 conjugate (16225; EMD Millipore; 1:500).

Image acquisition

Embryos were mounted in VECTASHIELD, and all imaging was conducted at 25°C. Fixed fluorescent images were acquired using an LSM 780 confocal microscope (ZEISS) with an AxioCam camera (MRm Rev.3 FireWire; ZEISS) using 20× (Plan Apochromat, air NA 0.8; ZEISS), 40× (Plan Apochromat, oil immersion, NA 1.4; ZEISS), and 63× (Plan Neufluor, oil immersion, NA 1.4; ZEISS) objectives, acquired using Zen black software (2012 version; ZEISS). Images were processed using ImageJ (National Institutes of Health).

Localization assessment

Stage 9 embryos, ∼3.5 h after egg laying (2-h collection) at 25°C, were collected, fixed, and stained with Rho1 or E-cadherin antibody. Images were acquired at 63× magnification using the LSM 780 confocal microscope as described above. For cortical intensity measurements, mean intensities of five 72-pixel regions of the midgut and germ cell cortices were taken using ImageJ. The midgut signal intensity was used for normalizing the Rho1 or E-cadherin staining within each embryo. At least six embryos were analyzed per genotype. The mean wild-type cortical intensity was set to 1, and the rest of the intensities were normalized to the wild type mean (Kunwar et al., 2008).

Polarization localization measurements were done in ImageJ. A 10-µm-wide (approximately one cell diameter) region encompassing the full width of the germ cell cluster (35–50 µm) was measured (Fig. 3 G). Fluorescent intensity measures across the full region were measured. The fluorescent intensities were normalized to the mean intensity per embryo. The centers of individual plots of five embryos were aligned and histogram plotted (Fig. 3 G). Representative images are of a single Z plane. Heat maps of the Rho1 fluorescent intensity were generated using the ImageJ "Fire" lookup table.

Maximum projections

With the exception of localization figures, images are 3D projections of multiple Z stacks. Reconstructions were composed using the maxi-

mum-intensity 3D reconstruction function in ImageJ. Outlines of midgut (Fig. 6) and gonad were made using Illustrator (Adobe).

Overlay projections

The outlining mask of the midgut (Fig. 2) was made using Hindsight staining and phalloidin to determine cell outlines. This image outline was projected over the confocal image to indicate which germ cells were within the midgut confines. All processes were completed using ImageJ.

PGC labeling by PAGFP

Stage 5 embryos of wild type, *wunen* mutants, *tre1*$^{-/-}$ mutants with *tre1*$^{+}$, *NRY*$^{-}$, and *NPIIY*$^{-}$ transgenes were analyzed. These also expressed mCherry::Vasa to visualize all germ cells and *nanos*Gal4::VP16 driving *UASp-PAGFP-αTub84B* for photoactivation (for crosses, see Table S1). Embryos were dechorionated in 50% bleach for 2 min and mounted on a glass coverslip, dorsal side toward the coverslip, with heptane glue and covered with halocarbon oil (HC-700) to avoid desiccation. Photoactivations were performed on ZEISS LSM 780 confocal microscope using a 20× objective, NA 0.8, with a 512 × 512 scan area and 3× zoom. We photoactivated a region of interest (ROI) that encompasses a single cell using a 405-nm, 25-mW laser at ∼75% power, pixel dwell of 1.61 µs, and 160 iterations. A range of one to four lateral-most cells were activated per embryo (Slaidina and Lehmann, 2017). After photoactivation, embryos were allowed to develop at 25°C in halocarbon oil on the coverslip and imaged at stage 12+. Activated cells in each embryo were scored as left or right side. For each genotype, at least 20 activated cells were scored. Embryos that were in the incorrect orientation, died, or did not contain at least one photoactivated cell were removed from analysis. Activated cells that remained in the center of the embryo were also not included in final analysis (see Table S3). Images were taken using minimal laser power to prevent photobleaching and cellular damage. For better visualization of germ cells, brightness was increased using ImageJ.

Two-photon live imaging

Embryos were collected at 25°C and dechorionated with 50% bleach for 3 min. Embryos were then mounted in halocarbon oil on an oxygen-permeable membrane (YSL Inc.) and covered with a 1.5-µm coverslip. Live imaging of germ cell migration was performed on an Ultima multiphoton system (Prairie Technologies) with an Olympus BX-51WI microscope equipped with a pulsed 4-W Ti:sapphire Chameleon laser (Coherent) with a custom Olympus BX2 filter cube (bandpass emission filter ET510/50m-2p, bandpass emission filter ET575/50m-2p, dichroic T550LPXS) controlled by PrairieView software (Prairie Technologies). The objective used was 40× oil (U Plan Fluorite, oil, 1.3 NA; Olympus).

An ROI was used that encompassed the region of germ cell migration. Stacks were 3 µm apart and taken every 60 or 90 s if longer samples were imaged. Movies were composed using Imaris software (Imaris x64 version 7.7.2) with a frame rate of 10 frames/s. Stills were processed using the same Imaris software.

Protein expression analysis

Embryos were collected within 2 h of egg laying and allowed to age an additional 2 h, so that germ cells are fully formed. Embryos were dechorionated with 50% bleach, frozen in liquid nitrogen, manually homogenized in 1% SDS buffer with β-mercaptoethanol, and boiled for 20 min. Following separation of protein extracts on 4%–12% Bis-Tris gradient gel (NuPAGE NP0321; Thermo Fisher Scientific), proteins were transferred to polyvinylidene fluoride membranes (162-0174; Bio-Rad Laboratories). Membranes were probed with the following antisera: mouse anti-Flag (F1804; Sigma-Aldrich; 1:10,000) and mouse anti α-Tubulin (T5168; Sigma-Aldrich; 1:10,000). Membranes were developed with an HRP-conjugated secondary antibody and enhanced chemiluminescence detection system (34080; Thermo Fisher Scientific).

Statistical analysis

P-values were calculated using ANOVA with Tukey's test for multiple comparisons. P-values and sample size are indicated on each figure. Each dot on the scatterplots represents an individual value, and all graphs display the mean and standard deviation. All graphs and statistical analyses were generated using Prism software (GraphPad Software).

Online supplemental material

Fig. S1 illustrates expression levels and localization of *tre1* wild-type and mutant transgenes. Fig. S2 depicts still images from Videos 1, 2, and 3 during transepithelial migration of wild type and mutants and quantification of migration defects apparent in live observation. Fig. S3 shows polarization measurements for E-cadherin in wild-type and domain mutant backgrounds as well as a quantification of migration defects after Gαo^{GDP} overexpression in germ cells. Fig. S4 summarizes a model for Wunen function in germ cell migration and death as well as quantification of Wunen-mediated germ cell death phenotypes in wild-type and *tre1* domain mutant backgrounds. Table S1 summarizes genotypes of all crosses performed for each figure. Table S2 shows primers used to generate each construct. Table S3 provides complete analysis of in vivo photoactivation experiments. Videos 1, 2, and 3 are live imaging of germ cell migration in wild-type, *tre1*^{scrt}, and *NPIIY*$^{-}$ embryos, respectively.

Acknowledgments

We would like to thank Dr. Andrew Tomlinson, Dr. Clark Coffman, and the Bloomington Drosophila Stock Center (National Institutes of Health grant P40OD018537) for fly stocks. The anti-Eya antibody (eya10H6) developed by Dr. Benzer and Dr. Bonini, the anti-rho1 (p1D9) antibody developed by Dr. Parkhurst, anti–DE-cadherin (DCAD2) developed by Dr. Uemura, anti-Sxl (M18) developed by Dr. Schedl, and anti-Hindsight (1G9) developed by Dr. Lipshitz were obtained from the Developmental Studies Hybridoma Bank, created by the Eunice Kennedy Shriver National Institute of Child Health and Human Development of the National Institutes of Health and maintained at the University of Iowa, Department of Biology. We would like to thank Michael Cammer from the New York University Medical Center microscopy core for imaging input, Alexey Soshnev for assistance with figures, Lionel Cristiaen for input, and Lehmann laboratory members for critical comments on the manuscript.

M.G. LeBlanc was a National Science Foundation Graduate Research Fellow. This work was supported by the National Institutes of Health (grant R37 HD49100 to R. Lehmann). R. Lehmann is a Howard Hughes Medical Institute Investigator.

The authors declare no competing financial interests.

Author contributions: M.G. LeBlanc and R. Lehmann designed the experiments. M.G. LeBlanc performed the experiments. M.G. LeBlanc and R. Lehmann wrote the manuscript.

Submitted: 9 December 2016
Revised: 28 April 2017
Accepted: 8 June 2017

References

Acharya, S., and S.S. Karnik. 1996. Modulation of GDP release from transducin by the conserved Glu134-Arg135 sequence in rhodopsin. *J. Biol. Chem.* 271:25406–25411. http://dx.doi.org/10.1074/jbc.271.41.25406

Ara, T., Y. Nakamura, T. Egawa, T. Sugiyama, K. Abe, T. Kishimoto, Y. Matsui, and T. Nagasawa. 2003. Impaired colonization of the gonads by

primordial germ cells in mice lacking a chemokine, stromal cell-derived factor-1 (SDF-1). *Proc. Natl. Acad. Sci. USA.* 100:5319–5323. http://dx.doi.org/10.1073/pnas.0730719100

Baeyens, A., V. Fang, C. Chen, and S.R. Schwab. 2015. Exit strategies: S1P signaling and T cell migration. *Trends Immunol.* 36:778–787. http://dx.doi.org/10.1016/j.it.2015.10.005

Barton, L.J., M.G. LeBlanc, and R. Lehmann. 2016. Finding their way: themes in germ cell migration. *Curr. Opin. Cell Biol.* 42:128–137. http://dx.doi.org/10.1016/j.ceb.2016.07.007

Borroto-Escuela, D.O., W. Romero-Fernandez, G. García-Negredo, P.A. Correia, P. Garriga, K. Fuxe, and F. Ciruela. 2011. Dissecting the conserved NPxxY motif of the M3 muscarinic acetylcholine receptor: critical role of Asp-7.49 for receptor signaling and multiprotein complex formation. *Cell. Physiol. Biochem.* 28:1009–1022. http://dx.doi.org/10.1159/000335788

Bréart, B., W.D. Ramos-Perez, A. Mendoza, A.K. Salous, M. Gobert, Y. Huang, R.H. Adams, J.J. Lafaille, D. Escalante-Alcalde, A.J. Morris, and S.R. Schwab. 2011. Lipid phosphate phosphatase 3 enables efficient thymic egress. *J. Exp. Med.* 208:1267–1278. http://dx.doi.org/10.1084/jem.20102551

Broihier, H.T., L.A. Moore, M. Van Doren, S. Newman, and R. Lehmann. 1998. zfh-1 is required for germ cell migration and gonadal mesoderm development in *Drosophila*. *Development.* 125:655–666.

Campos-Ortega, J.A., and V. Hartenstein. 1985. The Embryonic Development of *Drosophila melanogaster*. Springer, Berlin Heidelberg, Germany. http://dx.doi.org/10.1007/978-3-662-02454-6

Coffman, C.R., R.C. Strohm, F.D. Oakley, Y. Yamada, D. Przychodzin, and R.E. Boswell. 2002. Identification of X-linked genes required for migration and programmed cell death of *Drosophila melanogaster* germ cells. *Genetics.* 162:273–284.

Dawaliby, R., C. Trubbia, C. Delporte, M. Masureel, P. Van Antwerpen, B.K. Kobilka, and C. Govaerts. 2016. Allosteric regulation of G protein-coupled receptor activity by phospholipids. *Nat. Chem. Biol.* 12:35–39. http://dx.doi.org/10.1038/nchembio.1960

Doitsidou, M., M. Reichman-Fried, J. Stebler, M. Köprunner, J. Dörries, D. Meyer, C.V. Esguerra, T. Leung, and E. Raz. 2002. Guidance of primordial germ cell migration by the chemokine SDF-1. *Cell.* 111:647–659. http://dx.doi.org/10.1016/S0092-8674(02)01135-2

Gavis, E.R., and R. Lehmann. 1992. Localization of nanos RNA controls embryonic polarity. *Cell.* 71:301–313. http://dx.doi.org/10.1016/0092-8674(92)90358-J

Gavis, E.R., and R. Lehmann. 1994. Translational regulation of nanos by RNA localization. *Nature.* 369:315–318. http://dx.doi.org/10.1038/369315a0

Gether, U. 2000. Uncovering molecular mechanisms involved in activation of G protein-coupled receptors. *Endocr. Rev.* 21:90–113. http://dx.doi.org/10.1210/edrv.21.1.0390

Gibson, D.G., L. Young, R.-Y. Chuang, J.C. Venter, C.A. Hutchison III, and H.O. Smith. 2009. Enzymatic assembly of DNA molecules up to several hundred kilobases. *Nat. Methods.* 6:343–345. http://dx.doi.org/10.1038/nmeth.1318

Groth, A.C., M. Fish, R. Nusse, and M.P. Calos. 2004. Construction of transgenic *Drosophila* by using the site-specific integrase from phage phiC31. *Genetics.* 166:1775–1782. http://dx.doi.org/10.1534/genetics.166.4.1775

Hanyu-Nakamura, K., S. Kobayashi, and A. Nakamura. 2004. Germ cell-autonomous Wunen2 is required for germline development in *Drosophila* embryos. *Development.* 131:4545–4553. http://dx.doi.org/10.1242/dev.01321

Hauser, M.A., K. Schaeuble, I. Kindinger, D. Impellizzieri, W.A. Krueger, C.R. Hauck, O. Boyman, and D.F. Legler. 2016. Inflammation-induced CCR7 oligomers form scaffolds to integrate distinct signaling pathways for efficient cell migration. *Immunity.* 44:59–72. http://dx.doi.org/10.1016/j.immuni.2015.12.010

Izumi, Y., N. Ohta, A. Itoh-Furuya, N. Fuse, and F. Matsuzaki. 2004. Differential functions of G protein and Baz-aPKC signaling pathways in *Drosophila* neuroblast asymmetric division. *J. Cell Biol.* 164:729–738. http://dx.doi.org/10.1083/jcb.200309162

Kalatskaya, I., S. Schüssler, A. Blaukat, W. Müller-Esterl, M. Jochum, D. Proud, and A. Faussner. 2004. Mutation of tyrosine in the conserved NPXXY sequence leads to constitutive phosphorylation and internalization, but not signaling, of the human B2 bradykinin receptor. *J. Biol. Chem.* 279:31268–31276. http://dx.doi.org/10.1074/jbc.M401796200

Kamps, A.R., M.M. Pruitt, J.C. Herriges, and C.R. Coffman. 2010. An evolutionarily conserved arginine is essential for Tre1 G protein-coupled receptor function during germ cell migration in *Drosophila melanogaster*. *PLoS One.* 5:e11839. http://dx.doi.org/10.1371/journal.pone.0011839

Kassmer, S.H., D. Rodriguez, A.D. Langenbacher, C. Bui, and A.W. De Tomaso. 2015. Migration of germline progenitor cells is directed by sphingosine-1-phosphate signalling in a basal chordate. *Nat. Commun.* 6:8565. http://dx.doi.org/10.1038/ncomms9565

Katanaev, V.L., R. Ponzielli, M. Séméniva, and A. Tomlinson. 2005. Trimeric G protein-dependent frizzled signaling in *Drosophila*. *Cell.* 120:111–122. http://dx.doi.org/10.1016/j.cell.2004.11.014

Knaut, H., C. Werz, R. Geisler, C. Nüsslein-Volhard, and C. Tübingen Screen. Tübingen 2000 Screen Consortium. 2003. A zebrafish homologue of the chemokine receptor Cxcr4 is a germ-cell guidance receptor. *Nature.* 421:279–282. http://dx.doi.org/10.1038/nature01338

Kunwar, P.S., M. Starz-Gaiano, R.J. Bainton, U. Heberlein, and R. Lehmann. 2003. Tre1, a G protein-coupled receptor, directs transepithelial migration of *Drosophila* germ cells. *PLoS Biol.* 1:e80. http://dx.doi.org/10.1371/journal.pbio.0000080

Kunwar, P.S., H. Sano, A.D. Renault, V. Barbosa, N. Fuse, and R. Lehmann. 2008. Tre1 GPCR initiates germ cell transepithelial migration by regulating *Drosophila melanogaster* E-cadherin. *J. Cell Biol.* 183:157–168. http://dx.doi.org/10.1083/jcb.200807049

LeBlanc, M.G. 2016. GPCR signaling in migration: an in vivo perspective from *Drosophila* germ cells. PhD thesis. New York University, New York.

Lerit, D.A., and E.R. Gavis. 2011. Transport of germ plasm on astral microtubules directs germ cell development in *Drosophila*. *Curr. Biol.* 21:439–448. http://dx.doi.org/10.1016/j.cub.2011.01.073

McElwain, M.A., D.C. Ko, M.D. Gordon, H. Fyrst, J.D. Saba, and R. Nusse. 2011. A suppressor/enhancer screen in *Drosophila* reveals a role for wnt-mediated lipid metabolism in primordial germ cell migration. *PLoS One.* 6:e26993. http://dx.doi.org/10.1371/journal.pone.0026993

Mendelson, K., T. Evans, and T. Hla. 2014. Sphingosine 1-phosphate signalling. *Development.* 141:5–9. http://dx.doi.org/10.1242/dev.094805

Mitchell, R., D. McCulloch, E. Lutz, M. Johnson, C. MacKenzie, M. Fennell, G. Fink, W. Zhou, and S.C. Sealfon. 1998. Rhodopsin-family receptors associate with small G proteins to activate phospholipase D. *Nature.* 392:411–414. http://dx.doi.org/10.1038/32937

Molyneaux, K.A., H. Zinszner, P.S. Kunwar, K. Schaible, J. Stebler, M.J. Sunshine, W. O'Brien, E. Raz, D. Littman, C. Wylie, and R. Lehmann. 2003. The chemokine SDF1/CXCL12 and its receptor CXCR4 regulate mouse germ cell migration and survival. *Development.* 130:4279–4286. http://dx.doi.org/10.1242/dev.00640

Mukherjee, A., R.A. Neher, and A.D. Renault. 2013. Quantifying the range of a lipid phosphate signal in vivo. *J. Cell Sci.* 126:5453–5464. http://dx.doi.org/10.1242/jcs.136176

Murray, M.J., and R. Saint. 2007. Photoactivatable GFP resolves *Drosophila* mesoderm migration behaviour. *Development.* 134:3975–3983. http://dx.doi.org/10.1242/dev.005389

Ni, J.-Q., R. Zhou, B. Czech, L.-P. Liu, L. Holderbaum, D. Yang-Zhou, H.-S. Shim, R. Tao, D. Handler, P. Karpowicz, et al. 2011. A genome-scale shRNA resource for transgenic RNAi in *Drosophila*. *Nat. Methods.* 8:405–407. http://dx.doi.org/10.1038/nmeth.1592

Paksa, A., J. Bandemer, B. Hoeckendorf, N. Razin, K. Tarbashevich, S. Minina, D. Meyen, A. Biundo, S.A. Leidel, N. Peyrieras, et al. 2016. Repulsive cues combined with physical barriers and cell-cell adhesion determine progenitor cell positioning during organogenesis. *Nat. Commun.* 7:11288. http://dx.doi.org/10.1038/ncomms11288

Parés, G., and S. Ricardo. 2016. FGF control of E-cadherin targeting in the *Drosophila* midgut impacts on primordial germ cell motility. *J. Cell Sci.* 129:354–366. http://dx.doi.org/10.1242/jcs.174284

Patterson, G.H., and J. Lippincott-Schwartz. 2002. A photoactivatable GFP for selective photolabeling of proteins and cells. *Science.* 297:1873–1877. http://dx.doi.org/10.1126/science.1074952

Probst, W.C., L.A. Snyder, D.I. Schuster, J. Brosius, and S.C. Sealfon. 1992. Sequence alignment of the G-protein coupled receptor superfamily. *DNA Cell Biol.* 11:1–20. http://dx.doi.org/10.1089/dna.1992.11.1

Pruitt, M.M., M.H. Lamm, and C.R. Coffman. 2013. Molecular dynamics simulations on the Tre1 G protein-coupled receptor: exploring the role of the arginine of the NRY motif in Tre1 structure. *BMC Struct. Biol.* 13:15. http://dx.doi.org/10.1186/1472-6807-13-15

Rasmussen, S.G., B.T. DeVree, Y. Zou, A.C. Kruse, K.Y. Chung, T.S. Kobilka, F.S. Thian, P.S. Chae, E. Pardon, D. Calinski, et al. 2011. Crystal structure of the β2 adrenergic receptor-Gs protein complex. *Nature.* 477:549–555. http://dx.doi.org/10.1038/nature10361

Renault, A.D., Y.J. Sigal, A.J. Morris, and R. Lehmann. 2004. Soma-germ line competition for lipid phosphate uptake regulates germ cell migration and survival. *Science.* 305:1963–1966. http://dx.doi.org/10.1126/science.1102421

Renault, A.D., P.S. Kunwar, and R. Lehmann. 2010. Lipid phosphate phosphatase activity regulates dispersal and bilateral sorting of embryonic germ cells in *Drosophila*. *Development.* 137:1815–1823. http://dx.doi.org/10.1242/dev.046110

Richardson, B.E., and R. Lehmann. 2010. Mechanisms guiding primordial germ cell migration: strategies from different organisms. *Nat. Rev. Mol. Cell Biol.* 11:37–49. http://dx.doi.org/10.1038/nrm2815

Sano, H., A.D. Renault, and R. Lehmann. 2005. Control of lateral migration and germ cell elimination by the *Drosophila melanogaster* lipid phosphate phosphatases Wunen and Wunen 2. *J. Cell Biol.* 171:675–683. http://dx.doi.org/10.1083/jcb.200506038

Scheer, A., F. Fanelli, T. Costa, P.G. De Benedetti, and S. Cotecchia. 1996. Constitutively active mutants of the α 1B-adrenergic receptor: role of highly conserved polar amino acids in receptor activation. *EMBO J.* 15:3566–3578.

Schwabe, T., R.J. Bainton, R.D. Fetter, U. Heberlein, and U. Gaul. 2005. GPCR signaling is required for blood-brain barrier formation in *Drosophila*. *Cell.* 123:133–144. http://dx.doi.org/10.1016/j.cell.2005.08.037

Schwartz, T.W., and T.P. Sakmar. 2011. Structural biology: snapshot of a signalling complex. *Nature.* 477:540–541. http://dx.doi.org/10.1038/477540a

Seifert, J.R.K., and R. Lehmann. 2012. *Drosophila* primordial germ cell migration requires epithelial remodeling of the endoderm. *Development.* 139:2101–2106. http://dx.doi.org/10.1242/dev.078949

Slaidina, M., and R. Lehmann. 2017. Quantitative differences in a single maternal factor determine survival probabilities among *Drosophila* germ cells. *Curr. Biol.* 27:291–297. http://dx.doi.org/10.1016/j.cub.2016.11.048

Starz-Gaiano, M., N.K. Cho, A. Forbes, and R. Lehmann. 2001. Spatially restricted activity of a *Drosophila* lipid phosphatase guides migrating germ cells. *Development.* 128:983–991.

Trzaskowski, B., D. Latek, S. Yuan, U. Ghoshdastider, A. Debinski, and S. Filipek. 2012. Action of molecular switches in GPCRs—theoretical and experimental studies. *Curr. Med. Chem.* 19:1090–1109. http://dx.doi.org/10.2174/092986712799320556

Ueno, K., M. Ohta, H. Morita, Y. Mikuni, S. Nakajima, K. Yamamoto, and K. Isono. 2001. Trehalose sensitivity in *Drosophila* correlates with mutations in and expression of the gustatory receptor gene Gr5a. *Curr. Biol.* 11:1451–1455. http://dx.doi.org/10.1016/S0960-9822(01)00450-X

Van Doren, M., A.L. Williamson, and R. Lehmann. 1998. Regulation of zygotic gene expression in *Drosophila* primordial germ cells. *Curr. Biol.* 8:243–246. http://dx.doi.org/10.1016/S0960-9822(98)70091-0

Venkatakrishnan, A.J., X. Deupi, G. Lebon, F.M. Heydenreich, T. Flock, T. Miljus, S. Balaji, M. Bouvier, D.B. Veprintsev, C.G. Tate, et al. 2016. Diverse activation pathways in class A GPCRs converge near the G-protein-coupling region. *Nature.* 536:484–487. http://dx.doi.org/10.1038/nature19107

Wang, J., X. Wu, N. Simonavicius, H. Tian, and L. Ling. 2006. Medium-chain fatty acids as ligands for orphan G protein-coupled receptor GPR84. *J. Biol. Chem.* 281:34457–34464. http://dx.doi.org/10.1074/jbc.M608019200

Yoshiura, S., N. Ohta, and F. Matsuzaki. 2012. Tre1 GPCR signaling orients stem cell divisions in the *Drosophila* central nervous system. *Dev. Cell.* 22:79–91. http://dx.doi.org/10.1016/j.devcel.2011.10.027

Yuan, S., S. Filipek, K. Palczewski, and H. Vogel. 2014. Activation of G-protein-coupled receptors correlates with the formation of a continuous internal water pathway. *Nat. Commun.* 5:4733. http://dx.doi.org/10.1038/ncomms5733

Zhang, N., J. Zhang, Y. Cheng, and K. Howard. 1996. Identification and genetic analysis of wunen, a gene guiding *Drosophila melanogaster* germ cell migration. *Genetics.* 143:1231–1241.

Zhu, S.Z., S.Z. Wang, J. Hu, and E.E. el-Fakahany. 1994. An arginine residue conserved in most G protein-coupled receptors is essential for the function of the m1 muscarinic receptor. *Mol. Pharmacol.* 45:517–523.